Piezocomposite and CMUT Arrays Assessment Through In Vitro Imaging Performances

M. Legros[1], C. Meynier[1, 2], R. Dufait[1], G. Férin[1] and F. Tranquart[2]
1. Vermon SA, 180 rue du Général Renault, Tours, France.
2. INSERM U619, CHRU Bretonneau, 2 boulevard Tonnellé, Tours, France.
m.legros@vermon.com

Abstract— Piezoelectric and Capacitive Micromachined Ultrasound Transducers (CMUT) are usually measured and compared in regards to acoustic and electro-acoustic performances. This paper is focused on the imaging performances of such transducers and propose a quantitative imaging assessment of B-mode images. In this purpose, fully integrated CMUT and piezocomposite-based probes were manufactured. Transducers were designed with close features (geometries, center frequency, interconnect and packaging) and plug on a clinical ultrasound system with a research interface. Major imaging performances (Speckle to Noise Ratio, Resolutions and contrast) of the probes are presented. Despite an environment dedicated to piezoelectric transducers, CMUT probe exhibits comparable image quality as compared to a state-of-the-art piezocomposite probe. Indeed, close resolutions are calculated, field of view is improved in phased-array imaging, and contrast is significantly improved.

Keywords : Quantitative image assessment, CMUT, piezocomposite based transducer.

I. BACKGROUND AND MOTIVATIONS

Medical ultrasound imaging is a specific imaging modality, based on the complex interactions of human tissues with ultrasound beams formed by transducer arrays. In order, to improve diagnostic, imaging equipment manufacturers make continued efforts to enhance image quality.

For instance, ultrasound transducer is a capital element for image quality, and many degrees of freedom can be tuned to optimize performances of piezocomposite (assembly, materials ...) or micromachined arrays (layers strategy, membranes topologies ...). But the repercussions on image quality of such degrees of freedom are not always strongly identified.

Furthermore, ultrasound images are well-known to be difficult to quantify with on-screen images. *In-vivo* assessment are sensitive to probe incidence or patient motions, and is obviously dependent of the subjective point of view of the observer. Same limitations can also be found with *in-vitro* images, as the observer interpretation is part of the assessment.

For these reasons, ultrasound imaging requires robust tools for objective image quality assessment. We developed a specific method for transducer improvement and design orientation in regards to imaging performances. Here, we focused on B-mode images, since it is currently the most used diagnostic modality in ultrasound imaging and which is widely used for other methods (3D reconstruction, harmonic, compound imaging...). Computerized algorithms have been implemented and validated to objectively analyze ultrasound images from *in-vitro* characterization.

Besides, CMUT transducers has been widely investigated in the last decade, and B-mode images have been presented. Nevertheless imaging performances haven't been yet quantitatively discussed.

II. EQUIPMENTS AND SET-UP

Several imaging parameters have been investigated, and we have chosen to build our assessment method with *in-vitro* images from ultrasound phantoms. *In-vitro* characterization can provide reproducible images, if the object and the transducer remain still. Ultrasound phantoms consist of the following components (Figure 1) :

- A tissue mimicking material, it has close mechanical properties as compared to human soft tissues (attenuation and scattering coefficients, speed of sound…). The material contains the following test structures:
- Cylindrical anechoic targets (or cysts) with different radius.
- Nylon wires (or line targets) located at different depth.
- Cylindrical grayscale targets with different backscattering strength in regard to the surrounding medium (-15 to 15dB).

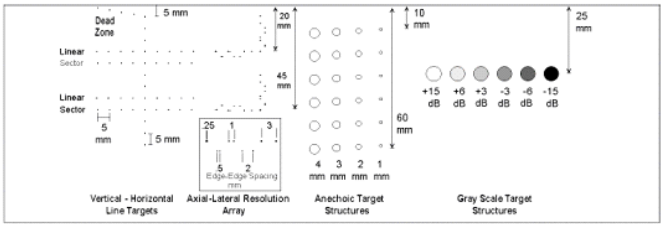

Figure 1 : Scheme of the ultrasound phantom used (http://www.atslabs.com)

A clinical ultrasound system with a research interface is used for data acquisition. The system handles data acquisition at different stages of the processing (RF post-beamformed, pre-scan converted, or scan converted) and allow access to a large variety of parameters. Scan-converted images will be preliminary used since these data corresponds to the on-screen images. The aim of the work is not to optimize the image quality, thus B-mode settings will be based on clinical presets. The imaging presets will be strictly fixed and TGC slidings potentiometers will be set to middle positions. Speed of sound is set to those of the phantom (1450 m/s), deduced by

acquiring raw data and observing wire targets at known distances. Look Up Table (LUT) can be chosen linear to have a pure logarithmic relation between echo voltage and pixel values [4]. For the images required for characterization, 5 acquisitions are recorded at different positions parallel to the xOz plane and will be used to get measurement deviations. CMUT probes have lower sensitivity than our piezocomposite based arrays; the system gain is thus adjusted for both probes in order to reach the same mean speckle level μ_S . The criterion μ_S is estimated from the same region of the tissue mimicking phantom and by averaging all pixel values.
In order to always ensure the same transducer incidence on the phantom, the probes will be held by a specific mechanical tool.

III. IMAGING PERFORMANCES PARAMETERS

We present thereafter the most representative parameters and detailed the way they've been developed using the Matlab computing environment (http://www.mathworks.com).

A. *Tissue mimicking : Speckle to Noise Ratio SNR*

The SNR is the ability to distinguish soft tissues from the electronic noise. Two complete images or region of interest (ROI) of the tissue mimicking are acquired successively. Between both images, speckle is identical whereas electronic noise is independent. The sum and difference of the images are computed to highlight signal and electronic noise. For each line i of the resulting matrices, the standard deviations σ_{sum} and σ_{diff} are calculated. Finally, $\sigma_{speckle}$, σ_{noise} and the SNR are then computed and displayed versus image depth [3] :

$$\sigma_{speckle}(i) = \frac{1}{2}\sqrt{\sigma_{sum}^2(i) - \sigma_{diff}^2(i)} \quad (1) \qquad \sigma_{noise}(i) = \frac{1}{\sqrt{2}}\sigma_{diff}(i) \quad (2)$$

$$SNR = 20 \times \log_{10}\left(\frac{\sigma_{speckle}}{\sigma_{noise}}\right) \quad (3)$$

Point-median and point-average filters are used to smooth the different curves. When SNR falls below 0dB, the electronic noise and speckle can't be dissociated. This threshold will be used to define the penetration depth.

B. *Line targets : resolutions assessment*

Resolution is the minimal distance of two adjacent objects aligned along a direction that the instrument is able to image distinctly. An image of the column wires is acquired and will be used to quantify axial and lateral resolutions at different depths. The algorithm localized all the wires, and defined for each target the maximum peak pixel intensity. From these maxima, axial and lateral profiles are plotted and are interpolated within the peak to increase accuracy of the measure. Axial and lateral resolutions are then calculated at Full Width Half Maximum taking into account a speckle mean level (Figure 2). The latter is evaluated considering the surrounding medium of the target [3].
The slice thickness can be also evaluated by a similar method [4]. We will not use this criterion here, since the transducers we will compare have identical center frequencies and no geometrical focus.

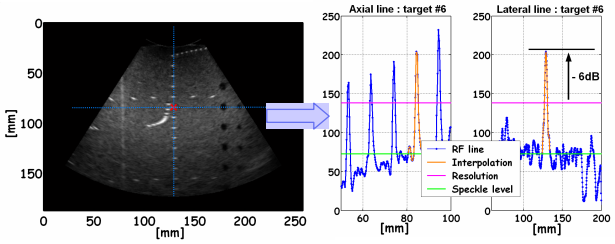

Figure 2 : Axial and lateral profile for a located wire target

C. *Anechoic targets : High-contrast sensitivity*

We use images of the anechoic targets to characterize the accuracy of the transducer to reproduce high-contrast targets with known shape.
A region of interest ROI embedding a single target of diameter D is selected. A numerical target with the same diameter is generated within an image of 1.5 D×1.5 D dimensions. The ROI selected had previously been interpolated to increase image resolution: this step is mandatory for small diameters cysts; in opposite case the numerical target created won't have a circle shape (low pixel size). Then 2D-matched filters are used to provide correlation between the ROI and the numerical target. The maximum point of correlation between both images is used as the center of the test object. The location of the object center allows the program to refocus the ROI as compared to its center within an image N with 1.5D×1.5D dimensions.

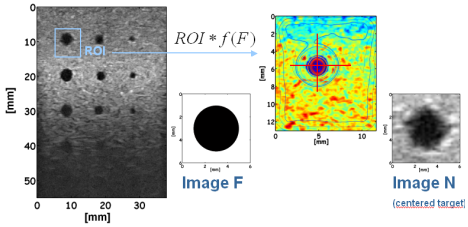

Figure 3 : Localisation of the target center with matched filter techniques

A correlation coefficient is then deduced from both images by the relation:

$$X_{COR} = \frac{\sigma_{N,F}}{\sigma_N \times \sigma_F} \quad (4)$$

Where σ is the standard deviation and $\sigma_{N,F}$ is the covariance.

D. *Grayscale targets : Contrast*

Contrast in B-mode imaging is the ability to distinguish two objects with close backscattering properties. The detection of the grayscale targets is performed with close manners as previously detailed. The protocol also refocus the target as compared to the grayscale center location in a new ROI within an image N of 1.5D×1.5D dimensions.
Two circles are then drawn, with diameters D± max(Rax,Rlat). Rax and Rlat are the axial and lateral resolutions calculated at the corresponding depth of the grayscale. The inside circle is used to compute mean and standard deviations within the target; the outside circle is employed to calculate the

surrounding speckle level and it standard deviation. The following parameters relative to contrast are then computed:

$$TCR = 20\times\log_{10}\left(\frac{\mu_{target}}{\mu_{speckle}}\right) \quad (5) \qquad TCR = 20\times\log_{10}\left(\frac{\mu_{target}}{\mu_{speckle}}\right) \quad (6)$$

$$CNR = \frac{\mu_{target} - \mu_{speckle}}{\sigma_{speckle}} \quad (7) \qquad CI_{SSIM} = \left(\frac{2\times\sigma_N\sigma_F}{\sigma_N^2+\sigma_F^2}\right) \quad (8)$$

Where μ is the mean pixel value, σ the standard deviation and F is a numerical target image with maximum dynamic range. CI_{SSIM} is widely used in image processing for measuring the contrast similarity between two images [5].

IV. PROGRAM VALIDATION

The pertinence of the computerized parameters have been assessed with numerical images obtained with Field II simulation program [1] [2]. 3D-numerical phantoms have been first built with the different targets required for characterization. Then RF-data are calculated and linear images were reconstructed. Table 1 gives results obtained for a linear array, (300µm pitch, 5 mm elevation, focused at 35 mm) obtained for a part of the imaging parameters. The different results were found in agreement with the trends usually meet in ultrasound imaging.

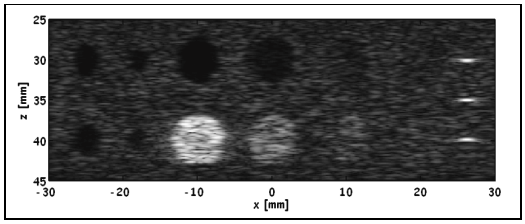

Figure 4 : Example of simulated phantom images

		Center frequency					
		5 MHz			7.5 MHz		
BW_r(%)		60	75	90	60	80	90
Resolutions	Axial	0.35	0.27	0.23	0.23	0.23	0.19
	Lateral	1.91	2.07	2.31	1.35	1.51	1.67
Correlation coefficient	4 mm diameter	0.64	0.61	0.59	0.65	0.64	0.61

Table 1 : Example of results obtained with a linear array exhibiting different frequencies and bandwidth.

The algorithms demonstrated their pertinence with numerical images and can thus be exploited with experimental images to link electro-acoustic and acoustic performances to imaging performances.

V. PROBES DESIGN

In this work, we will characterize fully integrated CMUT and piezocomposite probes dedicated to vascular imaging.
Insulation layer in front-face is mandatory for CMUT (moisture, patient isolation), however it impacts device performances (bandwidth, sensitivity). Some improvements are required to reach a wide bandwidth like observed from the same CMUT configuration without insulation layer (Figure 6).
B-mode imaging operates in emission-reception mode, and are driving by broadband excitation pulses. Thus, the CMUT pulse-echo response within these conditions is a key characterization part. The piezocomposite array was manufactured with the current state-of-the-art and to reach the closer pulse-echo response.

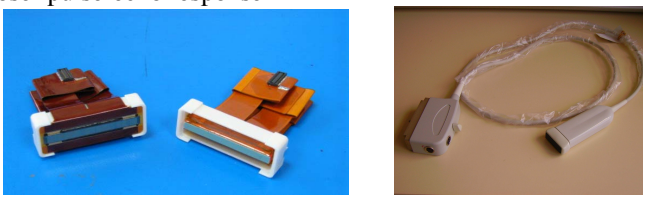

Figure 5 : Manufactured acoustic heads (CMUT and piezocomposite) before complete integration (left) and end-product (right)

In order to highlight accurately the imaging performances of both technologies, transducers are integrated with the same equipments (cable, printed circuit…).
The arrays have a 205µm pitch and a 3.5mm elevation, the Table 2 gives the electro-acoustical performances obtained at –6dB in pulse-echo measurement.

	fc [MHz]	BW [%]	Rax [ns]	Δf [MHz]
CMUT without insulation layer	8.5	115	96	3.5-13.4
CMUT with insulation layer	5.9	75	209	3.8-8.1
PIEZO	5.9	79	207	3.5-8.2

Table 2 : Performances measured in pulse-echo at -6dB

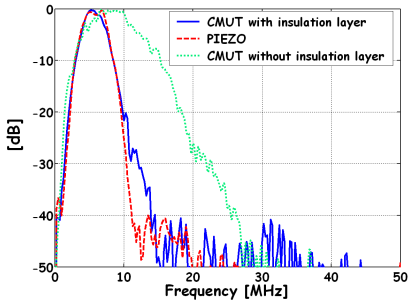

Figure 6 : Frequency responses of manufactured probes

VI. IMAGING CHARACTERIZATION

Both transducers are compared with following B-scan images:

- Linear images with different pulse frequencies (5 to 10 MHz)
- Spatial compound imaging with 6MHz pulse
- Phased-array sector images with 6MHz pulse (64 elements)
- Reconstructed images from RF-data with basic processing.

The measurements reliability of a parameter is computed by taking the maximum standard deviations from all the acquisitions and targets.

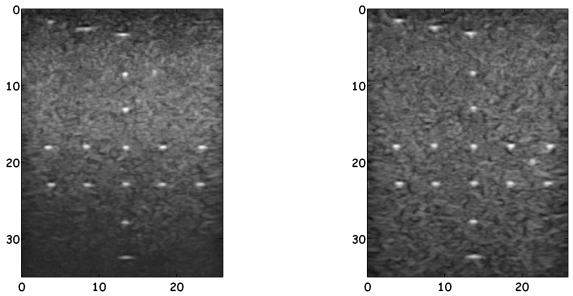

Figure 7 : Line targets images for a 8MHz excitation pulse with the same imaging preset : CMUT (left) and piezocomposite (right)

About SNR assessment, standard deviations of speckle versus depth show approximate values for both probes, indeed the system gain was adjusted to obtain the same mean grey level. However, Speckle to Noise Ratio with linear images isn't favorable to CMUT. This observation results in a penetration depth of 37mm for the CMUT against 40mm for the piezocomposite probe at 6MHz. The electronic noise resulting in a lower SNR for linear-scans is due to the interface CMUT-system which should be optimized. However, an important observation is done in phased-array steering: for wide angles, the SNR is improved for the CMUT probe as compared to the piezocomposite probe.

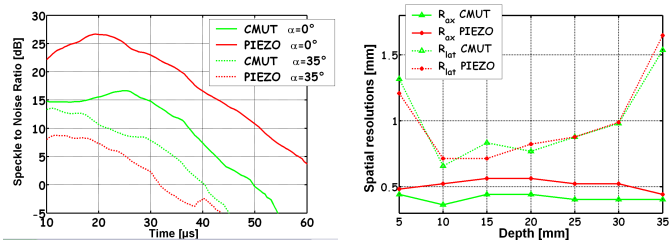

Figure 8 : SNR for phased-array images and spatial resolutions (6MHz pulse)

Resolutions results exhibits high performance arrays with axial resolutions less than 0.6mm at 6MHz. CMUT demonstrates a moderate impact in axial resolutions as compared to the piezoelectric probe with an improvement of 0,1 mm for a 6MHz excitation. CMUT exhibits fine lateral resolutions and are according to the average values, slightly better than the piezocomposite probe, but within the standard error of the measurement ($\Delta Rlat = 3.7x10^{-2}$ mm, $\Delta Rax = 3.0x10^{-2}$mm).

Anechoic targets assessment demonstrates that close properties are reached by the CMUT probe, despite an inferior ability for imaging small targets. The reduced sensitivity for high-contrast target is mainly due to the presence of electronic noise in the liquid filled targets.

	4mm	3mm	2mm	1mm
CMUT	0.72	0.69	0.60	0.40
PIEZO	0.75	0.71	0.64	0.61

Table 3 : Average values for the correlation coefficient with a 6MHz pulse

Grayscale targets exhibits close values for TCR, LSNR and CNR. Whereas, CI_{SSIM} foregrounds an important feature of the CMUT as compared to piezoelectric transducers. The contrast is improved with the micro-machined array until 12%.
For all the parameters considered, the images reconstructed from RF-data with the minimal data-processing (envelope detection, log compression and scan conversion), confirm the results obtained with all the on-screen images. Thus, the complex image processing of the system hasn't promoted one of both technologies.

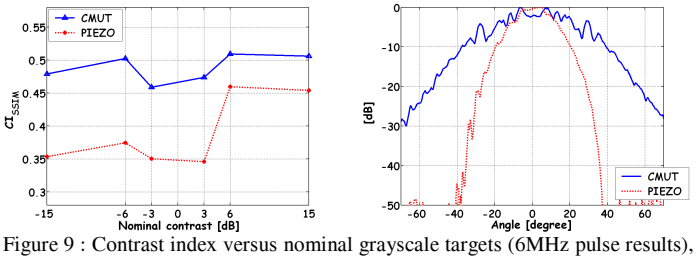

Figure 9 : Contrast index versus nominal grayscale targets (6MHz pulse results), and angular directivity measured at 6MHz

Although probes design is close, CMUT has attractive imaging features. The main reason results from the different principle of operation of CMUT providing large acoustic radiation fields(Figure 9).

VII. Conclusions

Our quantitative imaging method had demonstrated its accuracy for quantitative ultrasound imaging, and had allowed to highlight CMUT strengths for medical imaging. CMUT is fully compatible with conventional ultrasound system based for piezoelectric transducers. Despite an unfavorable environment (transducer integration and system dedicated for piezoelectric probes…), CMUT exhibits similar imaging performances as compared to piezoelectric transducers. Moreover, resolutions are slightly improved, contrast is significantly enhanced and field of view is superior.
Some improvements in CMUT chip integration and in insulation layer will improve once again the imaging performances of the technology, either on conventional ultrasound system or dedicated system.

References

[1] J.A. Jensen, "Field: A Program for Simulating Ultrasound Systems", Paper presented at the 10th Nordic-Baltic Conference on Biomedical Imaging Published in Medical & Biological Engineering & Computing, pp. 351-353, Volume 34, Supplement 1, Part 1, 1996.

[2] J.A. Jensen and N. B. Svendsen, "Calculation of pressure fields from arbitrarily shaped, apodized, and excited ultrasound transducers", IEEE Trans. Ultrason., Ferroelec., Freq. Contr., 39, pp. 262-267, 1992.

[3] Gibson NM, Dudley NJ, Griffith K., "A computerised quality control testing system for B-mode ultrasound", Ultrasound Med Biol, 2001;27:1697-711.

[4] Thijssen, J.M.; Weijers, G.; de Korte, C.L., "Objective Performance Testing and Quality Assurance of Medical Ultrasound Equipment", Ultrasonics Symposium, 2006. IEEE Volume , Issue , 2-6 Oct. 2006 Page(s):1625 - 1630.

[5] Z. Wang, A. C. Bovik, H. R. Sheikh and E. P. Simoncelli, "Image quality assessment: From error visibility to structural similarity", IEEE Transactions on Image Processing, vol. 13, no. 4, pp. 600-612, april 2004.

[6] Browne JE, Watson AJ, Gibson NM, Dudley NJ, Elliott AT. , "Objective measurements of image quality". Ultrasound Med. Biol. 2004; 30:229-37

[7] J. M. Thijssen, M. C. van Wijk, and M. H. Cuypers, "Performance testing of medical echo/Doppler equipment," Eur. J. Ultrasound,vol. 15, no. 3, pp. 151–164, Oct. 2002.